

1 **SUPPLEMENTAL MATERIAL FOR:**

2  
3  
4 **Title:** *Streptococcus mutans* requires mature rhamnase-glucose polysaccharides  
5 for proper pathophysiology, morphogenesis and cellular division

6  
7 **Authors:** Christopher J. Kovacs<sup>1‡</sup>, Roberta C. Faustoferri<sup>2</sup>, Andrew P. Bischer<sup>1</sup>,  
8 Robert G. Quivey Jr.<sup>1, 2, #</sup>

9 <sup>1</sup> Department of Microbiology & Immunology, Box 672

10 <sup>2</sup> Center for Oral Biology, Box 611

11 University of Rochester School of Medicine and Dentistry

12 Rochester, NY 14642

13  
14 #Corresponding author: Robert G. Quivey, Jr.  
15 Department of Microbiology & Immunology and  
16 Center for Oral Biology  
17 University of Rochester School of Medicine &  
18 Dentistry  
19 Rochester, NY 14642  
20 Telephone: 585-275-0382  
21 Email: Robert\_Quivey@urmc.rochester.edu

22  
23 ‡ Present address: Christopher J. Kovacs  
24 Department of Chemistry and Life Science  
25 United States Military Academy  
26 West Point, NY 10996  
27

## 28 **SUPPLEMENTAL EXPERIMENTAL PROCEDURES**

29

### 30 *Growth curves*

31 Growth rates were determined using a Bioscreen C plate reader (Growth  
32 Curves USA, Piscataway, NJ). Overnight cultures of *S. mutans* and mutant  
33 strains grown in BHI medium were subcultured into fresh BHI medium and  
34 incubated at 37°C in a 5% (v/v) CO<sub>2</sub>/95% air atmosphere until cultures reached  
35 an OD<sub>600</sub> of 0.3. A 10 µL aliquot was used to inoculate wells of a microtiter plate  
36 containing 300 µL test medium. A mineral oil overlay was added to wells to  
37 create a microaerobic environment. Assays were performed at 37°C (unless  
38 indicated differently) and OD<sub>600</sub> was continually read at 30 minute intervals  
39 following 10 seconds of shaking at medium amplitude. Assays were performed  
40 in three independent experiments with 5 replicates each and are displayed as  
41 mean OD<sub>600</sub> values ±SD. Generation times were calculated using the formula  
42  $0.3/[(N-N_0)/(T-T_0)]$ , where N represents the mean OD<sub>600</sub> value at the end of  
43 exponential phase and N<sub>0</sub> represents the mean OD<sub>600</sub> at the beginning of  
44 exponential phase. T and T<sub>0</sub> refer to the times in minutes that correspond to the  
45 OD<sub>600</sub> values for N and N<sub>0</sub>, respectively. Statistical significance ( $p \leq 0.001$ ) was  
46 determined by pairwise comparison using Student's *t*-test.

47

### 48 *Minimum inhibitory concentration (MIC) testing*

49 MIC testing was performed as per Clinical and Laboratory Standards  
50 Institute guidelines to assess antimicrobial efficacy of ampicillin, oxacillin,  
51 ceftriaxone, vancomycin, bacitracin, tunicamycin, nisin, cycloserine and

52 kanamycin against *S. mutans* UA159,  $\Delta rgpE$ ,  $rgpE^+$ ,  $\Delta rgpF$ ,  $rgpF^+$  and  $\Delta rgpG$   
53 (Clinical Laboratory Standards Institute, 2018). Briefly, two-fold serial dilutions of  
54 test article were made across wells of a 96-well microtiter plate in 100  $\mu$ l of BHI  
55 medium, to which 100  $\mu$ l of BHI containing  $\sim 3.0 \times 10^5$  cells were added. Plates  
56 were incubated overnight at 37°C in a 5% (v/v) CO<sub>2</sub>/95% air atmosphere and  
57 MIC values were determined as the lowest concentration within a dilution  
58 scheme that lacked evident growth. Data are derived from consensus MIC  
59 values of three independent experiments, performed in triplicate.

60

#### 61 *Antibiotic drug combinations and isobolograms*

62 Combination indices of tunicamycin and ampicillin co-administration  
63 against *S. mutans* UA159,  $\Delta rgpE$ ,  $rgpE^+$ ,  $\Delta rgpF$ ,  $rgpF^+$  and  $\Delta rgpG$  displayed as  
64 isobolograms (Zhao *et al.*, 2004). On the plots, connecting diagonal solid lines  
65 correspond to the MIC of tunicamycin (Y-axis) and the MIC of ampicillin (X-axis),  
66 respectively. Plotted points connected by dotted lines represent combinatorial  
67 MIC values (used to calculate the FIC). Points that fall on the solid line  
68 demonstrate indifferent effects of drug concentration combinations, those above  
69 the line are antagonistic, while points below the line show synergistic interactions  
70 of drugs. Data are derived from consensus MIC values of two independent  
71 experiments, performed in triplicate.

72

73

74

75 *Quantitative real-time PCR (qRT-PCR)*

76 RNA was extracted from three independent overnight batch cultures of  
77 bacteria, according to previously described methods (Abranches *et al.*, 2006,  
78 Baker *et al.*, 2014). The High Capacity cDNA Reverse Transcription kit (Applied  
79 Biosystems, Carlsbad, CA) was used to generate cDNA from RNA samples  
80 using random primers. Primers specific to genes of interest (listed in Table S3)  
81 were used with Power SYBR Green Master Mix (Applied Biosystems) and  
82 reactions were carried out in a Step One Plus Real-time PCR System (Applied  
83 Biosystems). The mRNA copy number was quantified based on a standard curve  
84 of PCR products for specific gene targets. Statistical significance ( $p \leq 0.05$ ) was  
85 determined by pairwise comparison using Student's *t*-test.

86

87

88

89 **REFERENCES**

- 90 Abranches J, Candella MM, Wen ZT, Baker HV, Burne RA. 2006. Different roles  
91 of EIIABMan and EIIIGlc in regulation of energy metabolism, biofilm  
92 development, and competence in *Streptococcus mutans*. *J Bacteriol*  
93 188:3748-3756.
- 94 Baker, J.L., A.M. Derr, K. Karuppaiah, M.E. MacGilvray, J.K. Kajfasz, R.C.  
95 Faustoferri, I. Rivera-Ramos, J.P. Bitoun, J.A. Lemos, Z.T. Wen & R.G.  
96 Quivey, Jr., (2014) *Streptococcus mutans* NADH oxidase lies at the  
97 intersection of overlapping regulons controlled by oxygen and NAD<sup>+</sup>  
98 levels. *J Bacteriol* **196**: 2166-2177.
- 99 Clinical Laboratory Standards Institute (2018) Methods for dilution antimicrobial  
100 susceptibility tests for bacteria that grow aerobically; approved standard—  
101 10th ed. M07-A11. Clinical and Laboratory Standards Institute, Wayne,  
102 PA.
- 103 Zhao, L., M.G. Wientjes & J.L. Au, (2004) Evaluation of combination  
104 chemotherapy: integration of nonlinear regression, curve shift,  
105 isobologram, and combination index analyses. *Clin Cancer Res* **10**: 7994-  
106 8004.  
107

108 **SUPPLEMENTAL FIGURE LEGENDS**

109

110 **FIGURE S1: Disruption of RGP causes growth impairment in *S. mutans*.**

111 Cultures of *S. mutans* UA159 (■),  $\Delta rgpE$  (□),  $rgpE^+$  (■),  $\Delta rgpF$  (■),  $rgpF^+$  (■) and  
112  $\Delta rgpG$  (■) were grown (A) in BHI medium at 37°C, (B) in BHI medium at 42°C,  
113 (C) in BHI medium supplemented with 1% NaCl at 37°C, and (D) in BHI medium  
114 supplemented with 20% sorbitol at 37°C. Growth was assessed by measuring  
115 optical density at 600 nm in a Bioscreen C plate reader (as described in  
116 Experimental Procedures). Assays were performed in three independent  
117 experiments with 5 replicates each and are displayed as mean OD<sub>600</sub> values  
118 ±SD.

119

120 **FIGURE S2. Antibiotic combination treatment.** Susceptibilities of *S. mutans*

121 (A) UA159 (■), (B)  $\Delta rgpE$  (□), (C)  $rgpE^+$  (■), (D)  $\Delta rgpF$  (■), (E)  $rgpF^+$  (■) and (F)  
122  $\Delta rgpG$  (■) against combinations of tunicamycin and ampicillin were performed  
123 using methodology for fractional inhibitory concentration testing as described in  
124 Experimental Procedures. Data are plotted as isobolograms, with solid  
125 connecting diagonal lines correspond to the MIC of tunicamycin (Y-axis) and the  
126 MIC of ampicillin (X-axis), respectively. Plotted points connected by dotted lines  
127 represent combinatorial MIC values (used to calculate the FIC). Points that fall  
128 on the solid line demonstrate indifferent effects of drug concentration  
129 combinations, those above the line are antagonistic, while points below the line  
130 show synergistic interactions of drugs.

131

132 **FIGURE S3. Polar effects of *rgpE*, *rgpF* and *rgpG* deletion.** RNA was isolated  
133 from overnight batch cultures and used to measure expression of genes  
134 surrounding *rgpG* (A). Gene expression within the *rgp* operon was also  
135 measured for the  $\Delta$ *rgpE* strain (B) and the  $\Delta$ *rgpF* strain (C). Samples from three  
136 independent cultures were measured in triplicate and are represented as mean  
137 values  $\pm$  SD. Statistical significance was determined by pairwise comparison  
138 using Student's *t*-test (\*  $p \leq 0.05$ ).

139

140 **FIGURE S4. Growth characteristics of *rgp* mutant strains.** Representative  
141 images of overnight growth for *S. mutans* UA159,  $\Delta$ *rgpE*, *rgpE*<sup>+</sup>,  $\Delta$ *rgpF*, *rgpF*<sup>+</sup>,  
142  $\Delta$ *rgpG*, and the “*rgpG* reverse complement” mutants UA159+[*rgpG*<sup>+</sup>] and  
143 UA159+[*rgpG*<sup>+</sup>/ $\Delta$ *rgpG*] (“*G*<sup>+</sup>/ $\Delta$ *G*”) grown in liquid BHI medium. Strains harboring  
144 most severe RGP disruption tend to flocculate and settle to bottom of culture  
145 tube. Notably, the UA159+[*rgpG*<sup>+</sup>/ $\Delta$ *rgpG*] strain fails to display phenotypic  
146 restoration and resembles the  $\Delta$ *rgpG* mutant.

147

148 **FIGURE S5. Characterization of  $\Delta$ *rgpG* genetic complementation mutants.**

149 (A) Transcription of *rgpG* was determined by qRT-PCR using RNA isolated from  
150 an overnight batch culture of *S. mutans* UA159,  $\Delta$ *rgpG*, UA159+[*rgpG*<sup>+</sup>] and  
151 UA159+[*rgpG*<sup>+</sup>/ $\Delta$ *rgpG*] (“*G*<sup>+</sup>/ $\Delta$ *G*”). Samples from three independent cultures were  
152 measured in triplicate and are represented as mean values  $\pm$  SD. Statistical  
153 significance was determined by pairwise comparison using Student's *t*-test (\*  $p \leq$   
154 0.05) versus UA159. (B) Antibiotic selection plating of UA159,  $\Delta$ *rgpG*,

155 UA159+[*rgpG*<sup>+</sup>] and UA159+[*rgpG*<sup>+</sup>/ $\Delta$ *rgpG*] (“*G*<sup>+</sup>/ $\Delta$ *G*”) demonstrating expression  
156 of appropriate resistance cassettes. Erm = erythromycin, Kan = kanamycin.

157

158 **FIGURE S6. Characterization of  $\Delta$ *rgpE* genetic complementation mutant.**

159 (A) Transcription of *rgpE* was determined by qRT-PCR using RNA isolated from

160 an overnight batch culture of *S. mutans* UA159,  $\Delta$ *rgpE* and *rgpE*<sup>+</sup>. (B) Antibiotic

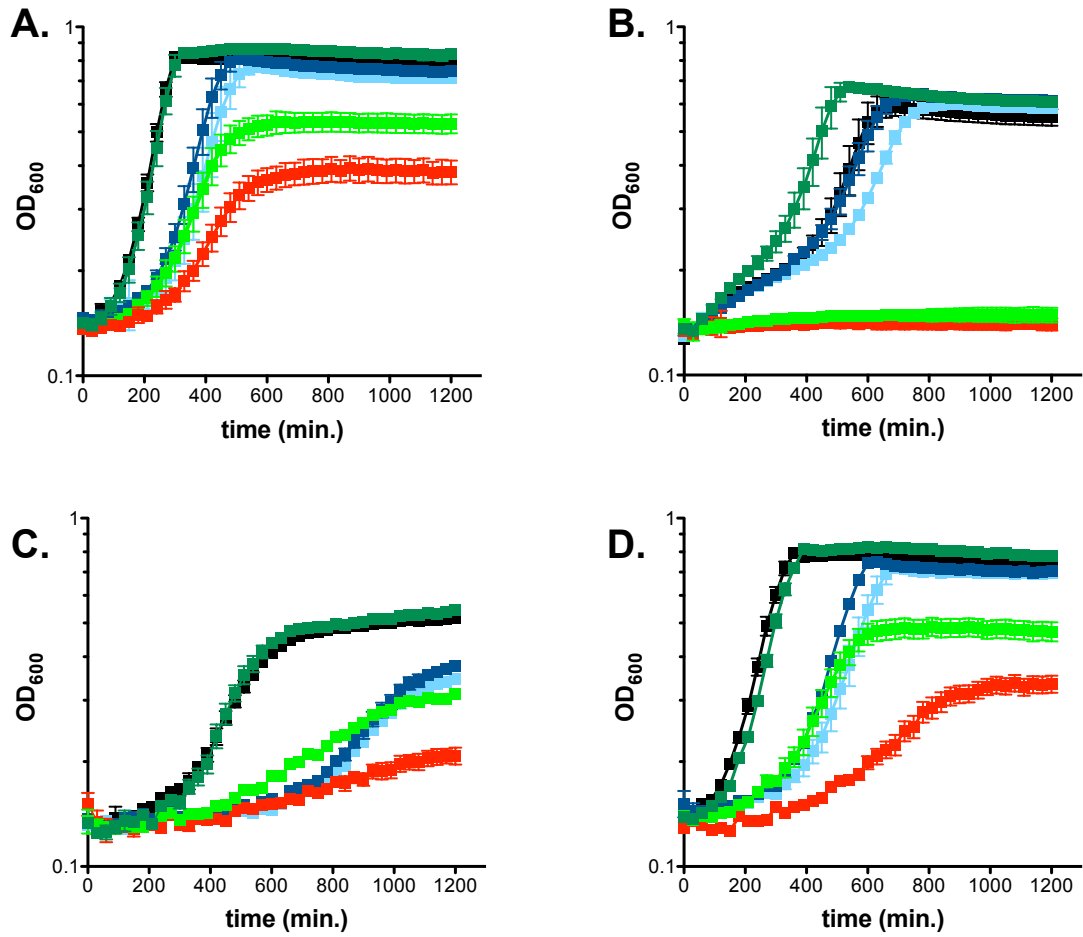
161 selection plating of UA159,  $\Delta$ *rgpE* and *rgpE*<sup>+</sup> demonstrating expression of

162 appropriate resistance cassettes. Erm = erythromycin, Kan = kanamycin.

163



164 **FIGURE S1**  
165  
166  
167



168  
169

170  
171  
172  
173  
174  
175  
176  
177  
178  
179

**Table S1** Calculated doubling times# of *S. mutans* UA159,  $\Delta$ *rgpE*, *rgpE*<sup>+</sup>,  $\Delta$ *rgpF*,

180 *rgpF*<sup>+</sup> and  $\Delta$ *rgpG*.

<i>S. mutans</i> strain	Doubling time (min.)							
	untreated, 37°C		untreated, 42°C		1% NaCl, 37°C		20% sorbitol, 37°C	
	Mean	SD	Mean	SD	Mean	SD	Mean	SD
UA159	83.6	1.9	346.6	6.5	118.8	5.9	342.0	12.6
$\Delta$ <i>rgpE</i>	147.0 <sup>†, a</sup>	8.9	482.5 <sup>†, c</sup>	16.8	183.1 <sup>†, d</sup>	7.0	694.2 <sup>†, f</sup>	24.6
<i>rgpE</i> <sup>+</sup>	141.5 <sup>†, a</sup>	10.1	372.0 <sup>†, c</sup>	12.6	164.3 <sup>†, d</sup>	10.9	640.9 <sup>†, f</sup>	26.6
$\Delta$ <i>rgpF</i>	244.8 <sup>†, b</sup>	31.2	NA		341.0 <sup>†, e</sup>	59.2	1419 <sup>†, g</sup>	98.1
<i>rgpF</i> <sup>+</sup>	82.2 <sup> b</sup>	3.4	258.4 <sup>†</sup>	47.3	120.9 <sup> e</sup>	6.1	311.6 <sup>†, g</sup>	14.6
$\Delta$ <i>rgpG</i>	438.1 <sup>†</sup>	49.6	NA		1005.6 <sup>†</sup>	124.9	NA	

# data derived from growth curves in Figure S2

†  $p \leq 0.01$  versus UA159

$p \leq 0.01$  where like letters are compared

181  
182  
183  
184

185  
186  
187  
188  
189  
190  
191  
192  
193  
194  
195

**Table S2** Minimum inhibitory concentration (MIC) testing for antibiotic susceptibilities.

197

antibiotic	MIC* ( $\mu\text{g ml}^{-1}$ )					
	UA159	$\Delta\text{rgpE}$	$\text{rgpE}^+$	$\Delta\text{rgpF}$	$\text{rgpF}^+$	$\Delta\text{rgpG}$
ampicillin	4	4	4	2	4	1
oxacillin	0.08	0.16	0.08	0.08	0.16	0.04
ceftriaxone	0.16	0.16	0.16	0.08	0.08	0.02
vancomycin	1	0.5	0.5	0.25	1	0.25
bacitracin	128	32	32	0.5	128	4
tunicamycin	1	4	4	16	1	8
nisin	512	512	512	32	512	64
cycloserine	512	512	512	256	512	256
kanamycin	128	64	128	8	128	16

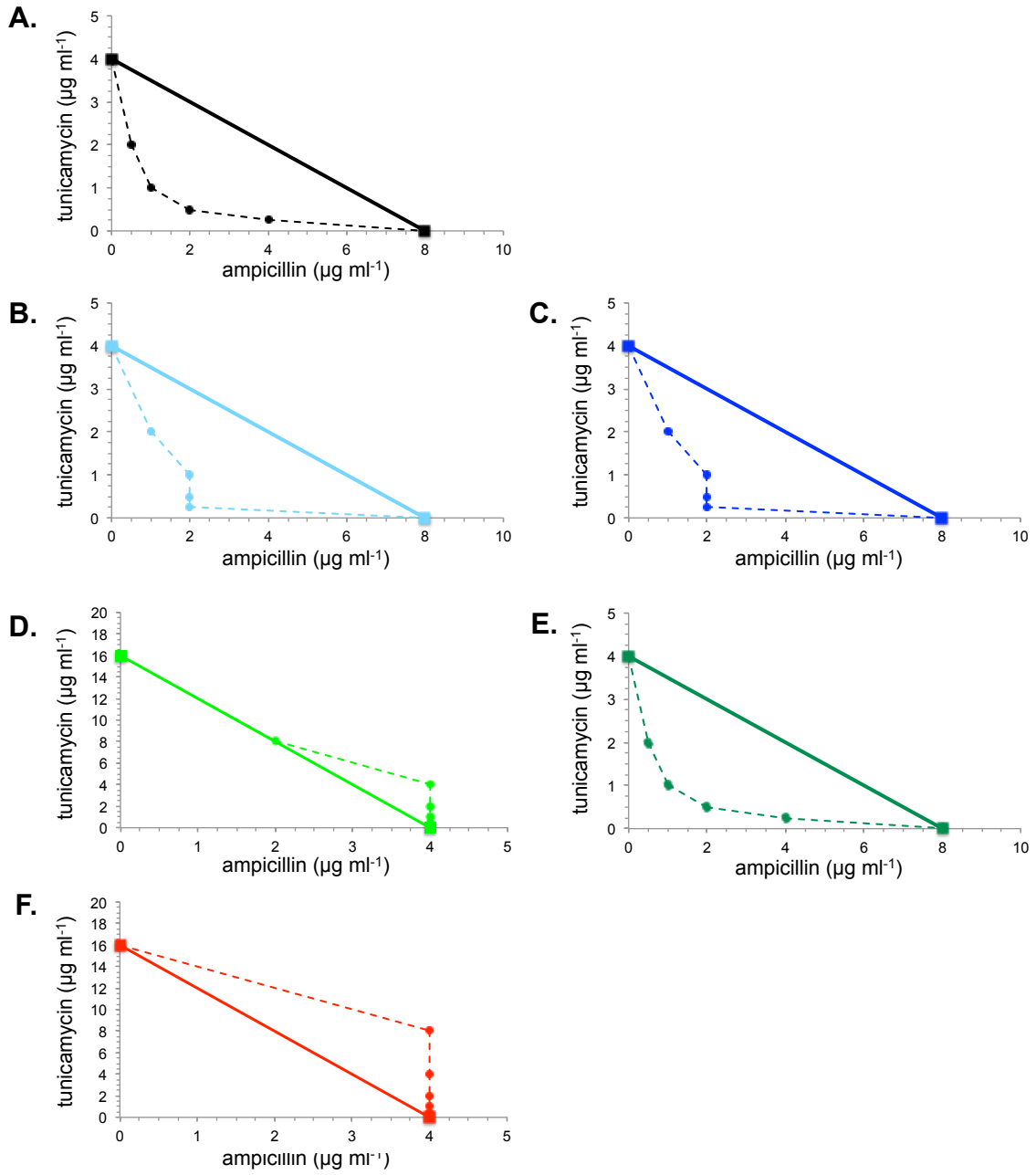
\* consensus value based on three independent experiments

Highlighted values were greater than 2-fold different compared to UA159 (green and red for reduced and enhanced susceptibility, respectively)

198  
199  
200  
201  
202  
203  
204  
205  
206  
207  
208  
209  
210  
211  
212

213  
214  
215  
216  
217  
218

**FIGURE S2**



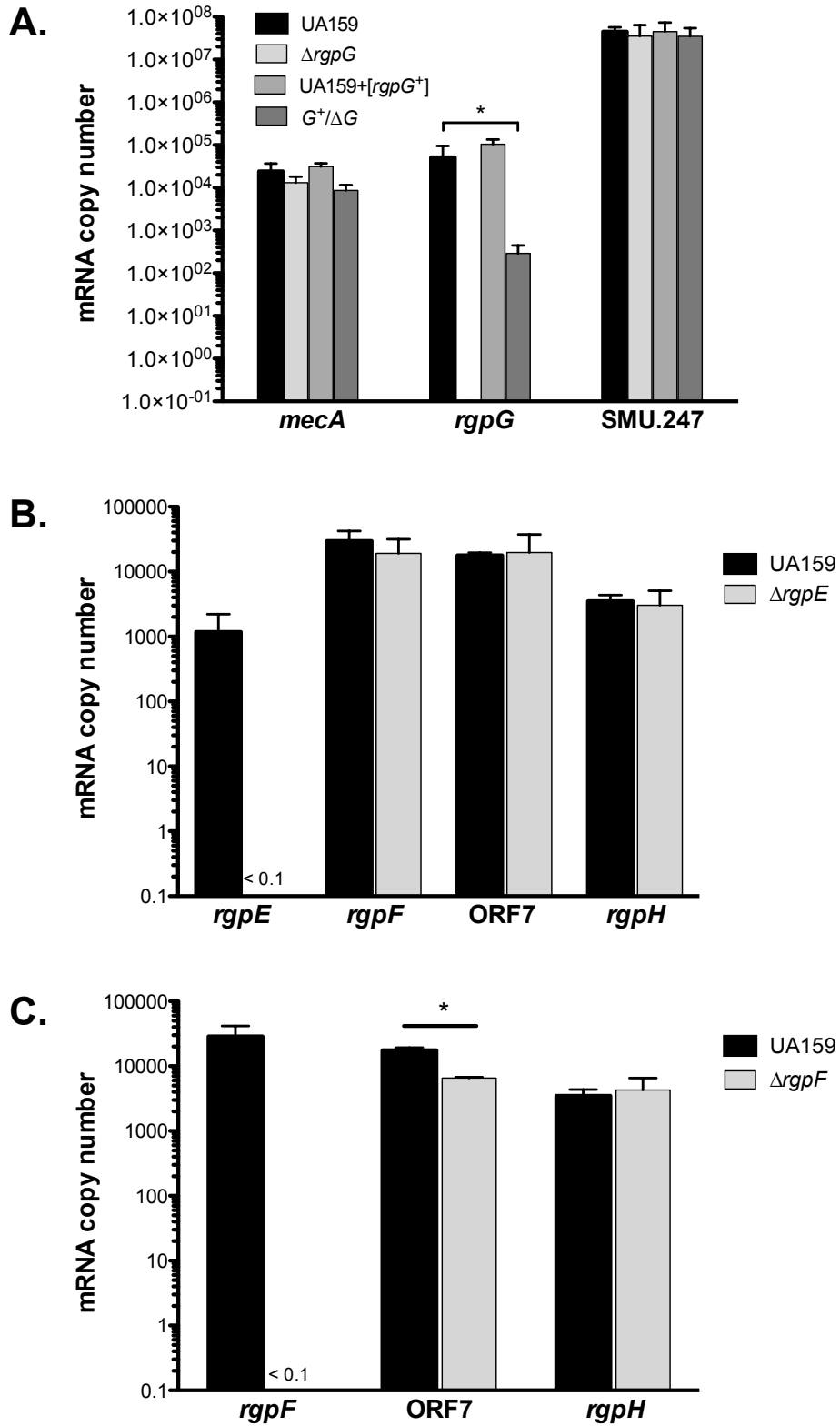
219  
220

221  
222  
223  
224  
225  
226  
227  
228  
229  
230  
231  
232  
233  
234  
235

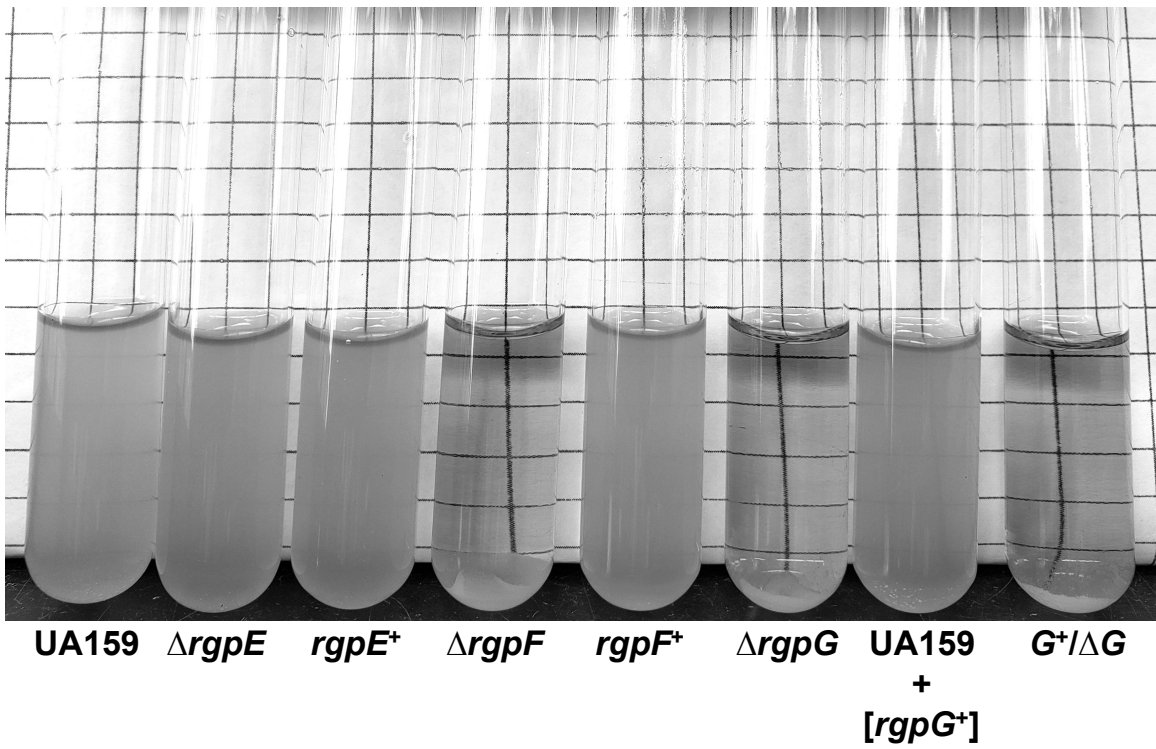
**TABLE S3.** Primers used for qRT-PCR.

Primer name	Sequence (5'-3')	Application
rgpE-qPCR-For	TGCTTCAACAGATCATTTCAG	forward primer for <i>rgpE</i> qPCR
rgpE-qPCR-Rev	ATCCAATAATCATCACCATCAC	reverse primer for <i>rgpE</i> qPCR
rgpF-qPCR-For	GCGAGATGGAATGGTCTT	forward primer for <i>rgpF</i> qPCR
rgpF-qPCR-Rev	CACGGTTGTTGGTCAATC	reverse primer for <i>rgpF</i> qPCR
ORF7-qPCR-For	GATGAGCCAAGTGATGTG	forward primer for ORF7 qPCR
ORF7-qPCR-Rev	TTATCTGTATAGGTCAGCAATC	reverse primer for ORF7 qPCR
rgpG-qPCR-For	GGTCCCATGCTCCACTTTAAT	forward primer for <i>rgpG</i> qPCR
rgpG-qPCR-Rev	CCAAACCATCCAAACCATCAATC	reverse primer for <i>rgpG</i> qPCR
mecA-qPCR-For	AGGAGTCTGACGCTTATCAC	forward primer for <i>mecA</i> qPCR
mecA-qPCR-Rev	CGTGTCTTTGTTCTCTACC	reverse primer for <i>mecA</i> qPCR
SMU.247-qPCR-For	TGCCATGCAATATCCGTCTG	forward primer for SMU.247 qPCR
SMU.247-qPCR-Rev	AGCGCTCTGCCATTTCTTC	reverse primer for SMU.247 qPCR

236  
237  
238  
239  
240  
241  
242  
243  
244  
245  
246  
247  
248  
249  
250  
251  
252  
253  
254

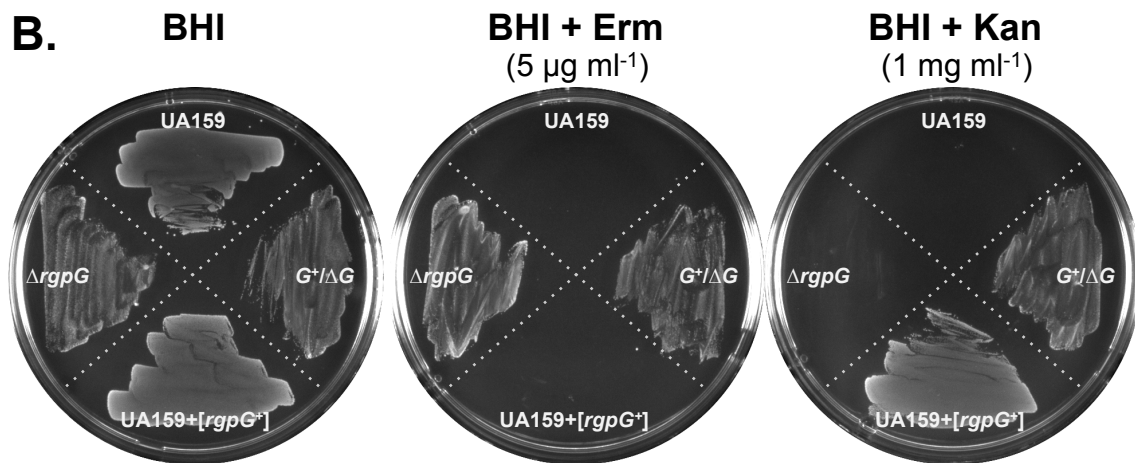
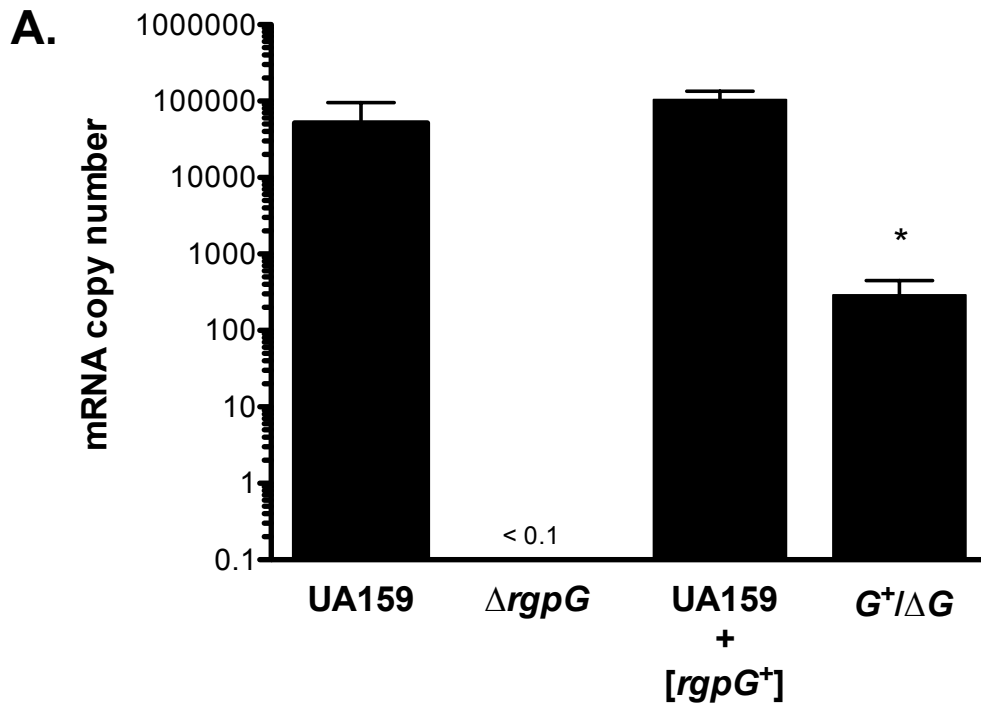


258 **FIGURE S4**  
259  
260  
261  
262  
263  
264  
265  
266  
267  
268  
269  
270  
271



272  
273  
274

275 **FIGURE S5**  
276  
277  
278  
279  
280



281  
282



